J|A|C|S
ARTICLES
Published on Web 03/30/2002

Benzdiynes (1,2,4,5-Tetradehydrobenzenes): Direct Observation by Wavelength-Selective Photolyses of Benzenetetracarboxylic Dianhydrides in Low-Temperature Nitrogen Matrixes

Tadatake Sato,* Sundaram Arulmozhiraja, Hiroyuki Niino, Shigekuni Sasaki,† Tohru Matsuura,† and Akira Yabe*

Contribution from the Photoreaction Control Research Center, National Institute of Advanced Industrial Science and Technology (AIST), 1-1-1 Higashi, Tsukuba, Ibaraki 305-8565, Japan

Received November 19, 2001

Abstract: Toward direct observation of benzdiynes, we investigated the wavelength-selective photolyses of five kinds of benzenetetracarboxylic dianhydride derivatives in nitrogen matrixes at 13 K. In the first step of the photolyses, all dianhydrides were converted into benzynedicarboxylic anhydrides with loss of CO and CO_2 upon irradiation at 308 nm. In the second step, the benzyne intermediates were photolyzed at 266 nm. In these photolyses, the generation of two kinds of benzdiynes, 3,6-difluoro-1,4-benzdiyne and 3,6-bis(trifluoromethyl)-1,4-benzdiyne, was confirmed by good correspondence between observed and calculated IR spectra. These benzdiynes were converted into the corresponding hexatriynes upon further irradiation at 266 nm. Benzdiynes were not observed in the photolyses of the other three dianhydrides: only hexatriynes were observed as major photoproducts. These results suggested that benzdiynes were generated first and then converted into hexatriynes and that the efficiency of the decomposition of benzdiynes depended on the substituents. The dynamics of the generation and decomposition of benzdiynes in the matrixes was analyzed by using a successive reaction scheme.

1. Introduction

The highly reactive intermediate *o*-benzyne (didehydrobenzene, C_6H_4) participates in a variety of organic chemical reactions and is among the most widely studied reactive intermediates in organic chemistry.[1,2] Its high reactivity originates from the strained triple bond in the benzene ring. Benzdiynes (tetradehydrobenzenes), on the other hand, are further unsaturated C_6H_2 chemical species having two triple bonds in the benzene ring. In contrast to the number of studies on *o*-benzyne, the number of studies on benzdiynes is small, probably because of their extraordinary lability owing to the high ring strain that arises from the two triple bonds. Because of their inherent instability, the benzdiynes are among the most challenging reactive intermediates to study. Although the existence of the benzdiynes was inferred as early as 1966 from the results of trapping experiments[3,4] and product analyses of the pyrolyses of dianhydrides,[5−7] direct spectroscopic proof of their existence was obtained only recently. During the intervening years, studies on benzdiynes were limited to theoretical studies.[8−10]

In 1997, we reported that the photolysis of 3,6-bis(trifluoromethyl)-1,2;4,5-benzenetetracarboxylic dianhydride in an argon matrix gave 3,6-bis(trifluoromethyl)-1,4-benzdiyne (**1a**).[11] This was the first direct experimental proof of the existence of a free benzdiyne structure as an intermediate in organic reactions. However, we could not detect the generation of unsubstituted benzdiyne (**1b**) under similar experimental conditions.[12,13] Why were we unable to observe the unsubstituted benzdiynes?

* To whom correspondence should be addressed. Fax: +81-298-61-4560. E-mail: sato-tadatake@aist.go.jp, akira.yabe@aist.go.jp.

† NTT Advanced Technology Corporation, Nihon-Seimei Musashino Building, 1-16-10, Naka-cho, Musashino-shi, Tokyo 180-0006, Japan.

(1) For instance: (a) Hoffmann, R. W. *Dehydrobenzene and Cycloalkynes;* Academic Press: New York, 1967. (b) Levin, R. H. In *Reactive Intermediates*; Jones, M., Moss, R. A., Eds.; John Wiley & Sons: New York, 1978; Vol. 1, Chapter 1.
(2) Radziszewski, J. G.; Hess, B. A., Jr.; Zahradnik, R. *J. Am. Chem. Soc.* **1992**, *114*, 52−57 and references therein.
(3) Hart, H.; Lai, C.-Y.; Nwokogu, G.; Shamouilian, S.; Teuerstein, A.; Zlotogorski, C. *J. Am. Chem. Soc.* **1980**, *102*, 6649−6651.
(4) Hart, H.; Raju, N.; Meador, M. A.; Ward, D. L. *J. Org. Chem.* **1983**, *48*, 4357−4360.
(5) Fields, E. K.; Meyerson, S. *J. Org. Chem.* **1966**, *31*, 3307−3309.
(6) Fields, E. K.; Meyerson, S. *Adv. Phys. Org. Chem.*, **1968**, *6*, 1−61.
(7) Fields, E. K. In *Organic Reactive Intermediates*; McManus, S. P., Ed.; Academic Press: New York, 1973; p 449.
(8) Adam, W.; Grimison, A.; Hoffmann, R. *J. Am. Chem. Soc.* **1969**, *91*, 2590−2599.
(9) Radom, L.; Nobes, R. H.; Underwood, D. J.; Li, W.-K. *Pure Appl. Chem.* **1986**, *58*, 75−88.
(10) Zahradnîk, R.; Hobza, P.; Burcl, R.; Hess, J. B. A.; Radziszewski, J. G. *J. Mol. Struct. (THEOCHEM)* **1994**, *313*, 335−349.
(11) Moriyama, M.; Ohana, T.; Yabe, A. *J. Am. Chem. Soc.* **1997**, *119*, 10229−10230.
(12) Moriyama, M.; Ohana, T.; Yabe, A. *Chem. Lett.* **1995**, 557−558.
(13) Moriyama, M.; Sato, T.; Uchimaru, T.; Yabe, A. *Phys. Chem. Chem. Phys.* **1999**, *1*, 2267−2274.

10.1021/ja017566n CCC: $22.00

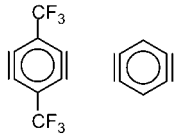

1a **1b**

In 1999, Bettinger, Schleyer, and Schaefer reported high-level ab initio and density functional theory (DFT) computational results for benzdiynes including **1a** and **1b**.[14] They argued that the IR band due to the asymmetrically coupled C≡C stretching mode in **1b** should be observable since this band had a predicted intensity of 8 km·mol^{-1} at the CCSD(T)/TZ2P level of computation. In addition to this band, three IR bands with intensities > 30 km·mol^{-1} (619 cm^{-1}, 157 km·mol^{-1}; 826 cm^{-1}, 33 km·mol^{-1}; 956 cm^{-1}, 35 km·mol^{-1}) were also predicted by this computation.[14] While the detection of a C≡C stretching band is an important topics in matrix-isolation studies on arynes,[2] the existence of intense IR bands is rather essential for the direct spectroscopic observation of **1b**.[15] Indeed, IR bands whose intensities were predicted to be >0.1 km·mol^{-1} were observed for *o*-benzyne in a 6 K neon matrix by Radziszewski et al.[2] We confirmed the generation of 1-naphthyne in an 11 K argon matrix by detecting most of the IR bands with intensities >5 km·mol^{-1} with our experimental setup.[16] Given these experimental results, direct observation of **1b**, that is, detection of IR bands with intensities >30 km·mol^{-1}, should be possible. However, these bands could not be detected in our experiments. Thus, there were likely other factors affecting the direct observation.

It should be noted that direct observation of benzdiyne depends on the concentration of benzdiynes in the matrix as well as the intensities of the IR bands. When benzdiynes are formed by stepwise decarboxylation and decarbonylation of benzenetetracarboxylic dianhydrides, several kinds of reactive intermediates that partially lose CO, CO_2, or both must be formed in the matrix.[12,13,17] Wavelength-selective irradiation is useful for controlling such consecutive photochemical reactions.[12,13,16−19] By careful choice of wavelength for the photolyses, photochemical reactions that would proceed simultaneously under broadband irradiation can be promoted consecutively. Consequently, the concentration of specific intermediates can be increased. In addition, wavelength-selective irradiation with high-intensity lasers is effective in driving photochemical reactions to completion, which facilitates analyses of IR spectra containing IR bands of several kinds of intermediates. Although we previously tried to detect **1a** and **1b** by the wavelength-selective photolyses of dianhydrides, we could detect only **1a**. The concentrations of these benzdiynes during the course of the wavelength-selective photolyses may be different owing to substituent effects. Substituent effects induced by kinetic factors or thermodynamic factors are possible. In the former case, the decomposition of benzdiynes by rearrangement may be suppressed, since a CF_3 group is more reluctant to migrate than a light H atom.[20] In the latter case, the electron-withdrawing effect of the CF_3 group may thermodynamically stabilize the benzdiyne with high electron density in an aromatic ring.

Against this backdrop, we investigated in detail the wavelength-selective photolyses of five kinds of dianhydrides with different substituents. In addition to the dianhydrides previously studied (**2a**, **2b**, and **2b-*d***), two kinds of anhydrides (**2c** and **2d**) were newly examined. The F group[21] (**2d**) and CF_3 group (**2c**) have often been used as substituents reluctant to migration.[22,23] The aims of the present study is two-fold: (1) to observe directly new benzdiyne derivatives and (2) to elucidate the factors affecting the possible direct observation of benzdiynes.

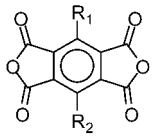

2a: $R_1 = R_2 = CF_3$
2b: $R_1 = R_2 = H$
2b-*d*: $R_1 = R_2 = D$
2c: $R_1 = CF_3$, $R_2 = H$
2d: $R_1 = R_2 = F$

2. Experimental Section

2.1. Materials. Dianhydrides **2b** and **2b-*d*** (97.8 atom % D) were purchased from Tokyo Kasei Co. and C/D/N Isotopes, respectively. The other dianhydrides were synthesized at NTT. The synthetic procedures for **2a** and **2c** are reported elsewhere.[24] Precursor **2d** was synthesized from 3,6-difluoro-1,2,4,5-tetracyanobenzene (SDS Biotech Co. Ltd.) as follows. The difluorotetracyanobenzene was hydrolyzed to the tetracarboxylic acid by an aqueous H_2SO_4 solution at 150 °C for 5 h and then converted into the dianhydride by treatment with acetic anhydride at 130 °C for 2 h. Dianhydride **2d**[25] was obtained with a yield of 27%.

All five dianhydrides were purified by sublimation before matrix isolation experiments.

2.2. Matrix Isolation Experiments. Matrix isolation experiments were performed with a closed-cycle helium cryostat (Air Products Displex CS-202). The pressure in the sample chamber was kept at 10^{-4}

(14) Bettinger, H. F.; Schleyer, P. v. R.; Schaefer, H. F. *J. Am. Chem. Soc.* **1999**, *121*, 2829−2835.
(15) Currently, we can identify the reactive intermediates generated in the matrix on the basis of the correspondence between the observed and calculated IR spectra, in particular, those calculated by the DFT method. The DFT method is known to be one of the most useful computational methods for predicting the vibrational spectra of various molecules.(Scott, A. P.; Radom, L. *J. Phys. Chem.* **1996**, *100*, 16502−16513., Wong, M. W. *Chem. Phys. Lett.* **1996**, *256*, 391−399., Kudo, S.; Takayanagi, M.; Nakata, M. *Chem. Phys. Lett.* **2000**, *322*, 363−370.). In this case, the identification is done by the comparing the whole spectral pattern. Therefore, detection of the IR bands ascribed to a specific functional group such as the C≡C bond stretching mode in *o*-benzyne is no longer essential for the identification. Instead, the existence of several groups of intense IR bands is indispensable for identifying the intermediates.
(16) Sato, T.; Moriyama, M.; Niino, H.; Yabe, A. *Chem. Commun.* **1999**, 1089−1090.
(17) Moriyama, M.; Yabe, A. *Chem. Lett.* **1998**, 337−338.
(18) Simon, J. G. G.; Münzel, N.; Schweig, A. *Chem. Phys. Lett.* **1990**, *170*, 187−192.
(19) Sato, T.; Niino, H.; Yabe, A. *J. Phys. Chem. A* **2001**, *105*, 7790−7798.
(20) Evans, R. A.; Wentrup, C. *J. Chem. Soc., Chem. Commun.* **1992**, 1062−1063.
(21) In determining the substituent effect of an F group, we have to consider both inductive and resonance effects. Basically, on one hand the F group works as a σ-electron-withdrawing substituent because of the high electronegativity of the F atom (Langenaeker, W.; Proft, F. D.; Geerlings, P. *J. Phys. Chem. A.* **1998**, *102*, 5944−5950; Jones, G. B.; Warner, P. M. *J. Am. Chem. Soc.* **2001**, *123*, 2134−3145). On the other hand, the F group often works as an electron-donating group owing to the resonance effect (Bibas, H.; Wong, M. W.; Wentrup, C. *Chem. Eur. J.* **1997**, *3*, 237−248).
(22) Breidung, J.; Bürger, H.; Kötting, C.; Kopitzky, R.; Sander, W.; Senzlober, M.; Thiel, W.; Willner, H. *Angew. Chem., Int. Ed. Engl.* **1997**, *36*, 1983−1985.
(23) O'Gara, J. E.; Dailey, W. P. *J. Am. Chem. Soc.* **1992**, *114*, 3581−3590.
(24) Matsuura, T.; Ishizawa, M.; Hasuda, Y.; Nishi, S. *Macromolecules* **1992**, *25*, 3540−3545.
(25) Spectroscopic data of **4d** are as follows: ^{13}C NMR (DMSO) δ 163, 2 (C=O), 153.0, 150.4 (C−F, $^1J_{CF}$ = 261 Hz) 124.7, 124.8, 125.0 ($^2J_{CF}$ = 8−15 Hz); FTIR (v/cm^{-1}) observed in an nitrogen matrix and predicted frequencies (cm^{-1}) and intensities (km·mol^{-1}): − (595, 7), 614w (607, 5), 753w (725, 7), 763m (736, 51), − (768, 4), 918s (897, 386), 940m (921, 119), 1186s, 1208w (1163, 724), 1312m (1287, 47), 1380w (1369, 13), 1508m (1479, 220), 1797vs, 1813m (1808, 1041), 1828m, 1834m, 1861m, 1873m, 1888m (1852, 413); MS *m*/*z* Observed 253.972 (M^+), Calculated 253.966.

to 10^{-5} Pa during the experiments. A CsI plate cooled to 13 K was used as a substrate, on which vaporized precursors were codeposited with nitrogen (99.9999%) at 11 K. The sample chamber of the cryostat had two pairs of windows: a pair of KBr windows for FTIR measurements and a pair of quartz windows for UV−vis measurements. With this sample chamber, the photoreaction in the matrix could be followed by FTIR and UV−vis spectroscopies simultaneously. The FTIR measurements were carried out on a Perkin-Elmer Spectrum-GXI spectrometer with a resolution of 1 cm^{-1}. UV−vis absorption spectra were measured with a Shimadzu UV-3100 spectrometer.

Wavelength-selective photoirradiation was carried out with the following nanosecond-pulsed lasers: (1) a XeCl excimer laser (308 nm: Lambda Physik Compex-102), whose repetition rate and laser fluence were 5 Hz and 3−4 $mJ\cdot cm^{-2}\cdot pulse^{-1}$, respectively; and (2) fourth harmonic generated (FHG) pulses of a Nd:YAG laser (266 nm: Lotis LS-2125 with a YHG-34 accessory), whose repetition rate and laser fluence were 10 Hz and ca. 3 $mJ\cdot cm^{-2}\cdot pulse^{-1}$, respectively. The fluence of the irradiation was kept constant in each batch.

2.3. Computational Methods. All DFT calculations were performed with the Gaussian 98 program package.[26] The geometries of the compounds were optimized by using the B3LYP method[27,28] in combination with the 6-31G* basis set. The nature of the stationary points was assessed by means of vibrational frequency analysis. Theoretical IR spectra were obtained by vibrational frequency analysis. For the benzdiynes, additional calculations using the cc-pVTZ basis set were executed for both the geometry optimization and the frequency analysis. A symmetry-broken spin-unrestricted method was adopted for the calculation of the benzdiynes since unstable solutions were obtained by the restricted method.[29,30] Vibrational frequencies predicted at the B3LYP/6-31G* level were scaled by 0.9614 on the basis of literature,[31] whereas vibrational frequencies predicted at the B3LYP/cc-pVTZ level were used without scaling. All calculations were done on the IBM RS/6000-SP system at the Tsukuba Advanced Computing Center (TACC).

3. Results and Discussion

3.1. Photolyses of Dianhydrides at 308 nm. Five kinds of dianhydrides were employed as precursors of benzdiynes. As the first step of our wavelength-selective photolyses, these precursors were photolyzed with a XeCl excimer laser (λ = 308 nm). Results for the photolysis of **2a** are described first. Precursor **2a** was sublimed at 85−90 °C, and codeposited with nitrogen on the cold substrate at 13 K, and then photolyzed. The photoreactions induced by irradiation were followed by FTIR and UV−vis spectroscopies. Upon irradiation, the IR bands of **2a** decreased and were gradually replaced by a set of new IR bands. The appearance of IR bands due to CO_2 (662 and 2347 cm^{-1}) and CO (2140 cm^{-1}) indicated decarboxylation and decarbonylation of **2a**. In general, an arenedicarboxylic anhydride is converted into the corresponding aryne by stepwise decarboxylation and decarbonylation. For instance, in the wavelength-selective photolysis of naphthalenedicarboxylic anhydride,[19] a cyclopropanone intermediate was initially formed by decarboxylation of the anhydride, and then decarbonylation of the cyclopropanone intermediate produced naphthyne. In the photolysis of phthalic anhydride to *o*-benzyne, Radziszewski et al. confirmed temporal formation of a cyclopropanone intermediate by the characteristic IR band at 1852 cm^{-1}, although decarboxylation and decarbonylation proceeded simultaneously.[2] In our previous report on the photolysis of **2a**,[11] we tentatively assigned the IR band at 1858 cm^{-1} to cyclopropanone intermediate **3a**.

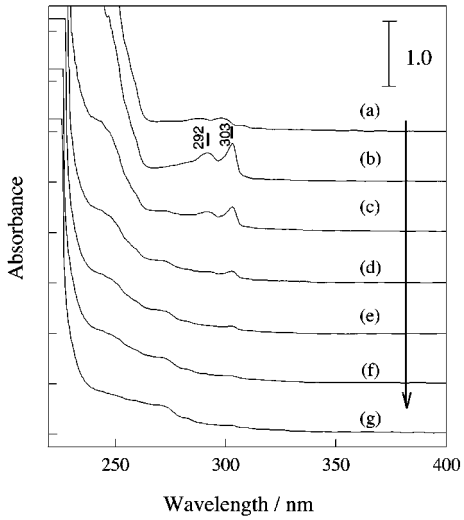

Figure 1. UV−vis absorption spectra of **2a** upon irradiation with a XeCl excimer laser (λ = 308 nm): (a) 0, (b) 600, (c) 3000, (d) 6000, (e) 12 000, (f) 24 000, and (g) 60 000 pulses.

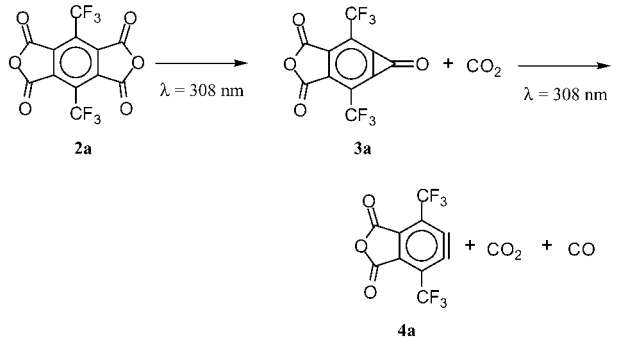

Participation of **3a** was suggested in the UV−vis absorption spectra (Figure 1). At the beginning of the irradiation, distinct absorption bands appeared at 303 and 292 nm (Figure 1b). These bands decreased gradually with irradiation, and finally disappeared. After prolonged irradiation, the UV−vis absorption spectra reached a photostationary state, where only structureless absorption was observed (Figure 1g). These results revealed that **3a** was temporally formed and then converted into **4a**.

The dynamics of the photochemical reactions from **2a** to **4a** could be studied by analyzing the intensities of the IR bands due to CO and CO_2. The concentration of CO_2 generated in the matrix must correspond to the total concentration of the photoproducts, in this case, **3a** and **4a**. On the other hand, the concentration of CO must be equal to that of **4a**. Therefore, a

(26) Frisch, M. J.; Trucks, G. W.; Schlegel, H. B.; Scuseria, G. E.; Robb, M. A.; Cheeseman, J. R.; Zakrzewski, V. G.; Montgomery, J. A., Jr.; Stratmann, R. E.; Burant, J. C.; Dapprich, S.; Millam, J. M.; Daniels, A. D.; Kudin, K. N.; Strain, M. C.; Farkas, O.; Tomasi, J.; Barone, V.; Cossi, M.; Cammi, R.; Mennucci, B.; Pomelli, C.; Adamo, C.; Clifford, S.; Ochterski, J.; Petersson, G. A.; Ayala, P. Y.; Cui, Q.; Morokuma, K.; Malick, D. K.; Rabuck, A. D.; Raghavachari, K.; Foresman, J. B.; Cioslowski, J.; Ortiz, J. V.; Baboul, A. G.; Stefanov, B. B.; Liu, G.; Liashenko, A.; Piskorz, P.; Komaromi, I.; Gomperts, R.; Martin, R. L.; Fox, D. J.; Keith, T.; Al-Laham, M. A.; Peng, C. Y.; Nanayakkara, A.; Gonzalez, C.; Challacombe, M.; Gill, P. M. W.; Johnson, B.; Chen, W.; Wong, M. W.; Andres, J. L.; Gonzalez, C.; Head-Gordon, M.; Replogle, E. S.; Pople, J. A. *Gaussian 98*, Revision A.9; Gaussian, Inc.: Pittsburgh, PA, 1998.
(27) Becke, A. D. *J. Chem. Phys.* **1993**, *98*, 5648−5662.
(28) Lee, C.; Yang, W.; Parr, R. G. *Phys. Rev. B* **1988**, *37*, 785−789.
(29) Arulmozhiraja, S.; Sato, T.; Yabe, A. *J. Comput. Chem.* **2001**, *22*, 923−930.
(30) Arulmozhiraja, S.; Sato, T.; Yabe, A. Submitted for publication.
(31) Scott, A. P.; Radom, L. *J. Phys. Chem.* **1996**, *100*, 16502−16513.

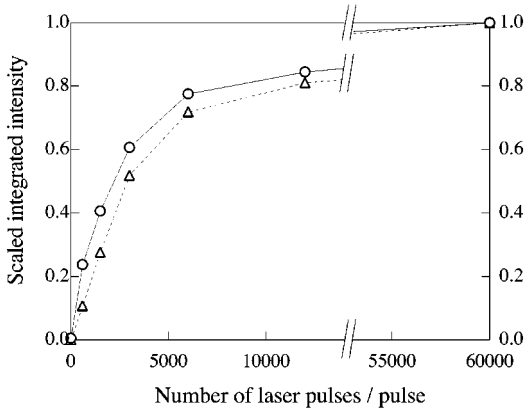

Figure 2. Change in the scaled integrated intensities of the IR bands due to CO_2 (circles) and CO (triangles) upon irradiation with a XeCl excimer laser (λ = 308 nm). Intensities are relative to the photostationary state (intensity at the photostationary state = 1), which was reached after irradiation with 60 000 pulses.

difference between the concentrations of CO_2 and CO indicates the existence of **3a**. Since **2a** was completely converted into **4a** at the photostationary state, the concentrations of CO and CO_2 at this state must be equal to the concentration of **4a**. Accordingly, the molar ratios of CO and CO_2 in the matrix could be estimated by scaling their IR intensities to those at the photostationary state (intensities at the photostationary state = 1). Figure 2 shows the molar ratios of CO_2 and CO during irradiation at 308 nm. At the beginning of the irradiation, the molar ratio of CO_2 was larger than that of CO, indicating the existence of **3a**.[32] Continued irradiation resulted in disappearance of the difference, indicating that **3a** had been completely converted into **4a**. The FTIR spectrum observed at the photostationary state is shown in Figure 3. The observed spectrum is in good agreement with the calculated IR spectrum of **4a**. No IR bands ascribed to other chemical species appeared in this spectrum, indicating that there was no side reactions. Thus, it was confirmed that more than 99% of the **2a** present initially was converted into **4a** upon irradiation at 308 nm.

The other dianhydrides (**2b**, **2b-*d***, **2c**, **2d**) behaved similarly to **2a** upon irradiation at 308 nm; that is, they were converted into the corresponding benzyne intermediates. The FTIR spectra observed at the photostationary state were depicted with computational results in the Supporting Information (Figures S5, S10, S15). These benzyne intermediates were identified on the basis of good agreement between the observed and calculated IR spectra. None of these intermediates showed further reaction upon continued irradiation at 308 nm. Except for difluorinated benzyne intermediate **4d**, they showed structureless UV−vis absorption spectra (Figure 1g). Figure 4 shows the UV−vis absorption spectrum of **4d**: prominent absorption bands were observed at 294, 282, and 272 nm. To clarify the origin of these UV−vis absorption bands, we examined the time-dependent (TD) DFT calculations of **2d** and **4d** (Figure 4b). These computational results showed that the prominent absorption bands of **4d** originated from the resonance effect of the fluorine group (see Supporting Information).

(32) The temporal formation and decomposition of **3a** were also confirmed by FTIR spectra. The FTIR spectrum of **3a** being in good agreement with the calculated result was depicted in the Supporting Information (Figure S3).

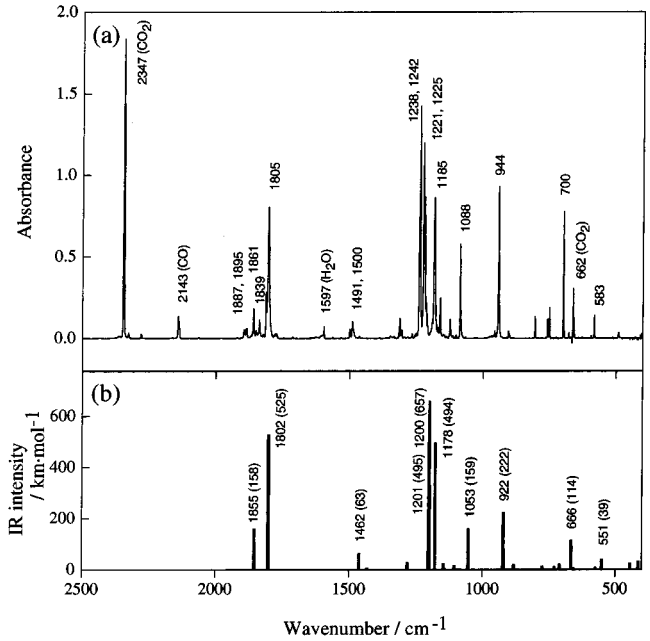

Figure 3. (a) FTIR absorption spectrum observed at the photostationary state upon irradiation of **2a** at 308 nm and (b) theoretical IR spectrum of **4a** calculated at the B3LYP/6-31G* level.

3.2. Photolyses of Benzyne Intermediates at 266 nm. 3.2.1. Photolysis of Bis(trifluoromethyl)benzynedicarboxylic Anhydride. To avoid inducing multiple reactions during irradiation, photolysis should be carried out under conditions as mild as possible, that is, at a wavelength as long as possible. We chose to use the FHG pulses of a Nd:YAG laser (266 nm) for the successive photolyses of the benzyne intermediates. All of the benzyne intermediates could be photolyzed at 266 nm, whereas they were stable upon irradiation at 308 nm. We first describe our experimental results for the photolysis of **4a** at 266 nm. Upon irradiation, we observed further increases in the intensities of the IR bands due to CO and CO_2, indicating decarboxylation and decarbonylation of **4a**. This photolysis is assumed to proceed as follows:

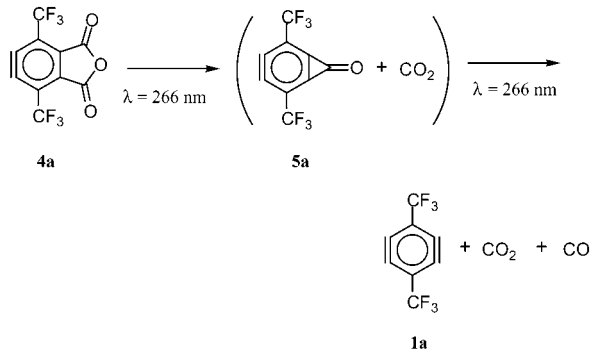

4a **5a** **1a**

The dynamic behavior of the intensities of the IR bands due to CO and CO_2 is shown in Figure 5. As in the case of 308 nm photolysis, the molar ratios of CO and CO_2 generated by 266 nm photolysis could be estimated by scaling their IR intensities to those at the photostationary state for 308 nm irradiation. The dynamics of the CO and CO_2 bands was almost the same (Figure 5), indicating that an anhydride group was removed from **4a** upon irradiation at 266 nm and that the concentration of the cyclopropanone intermediate **5a** was negligible.

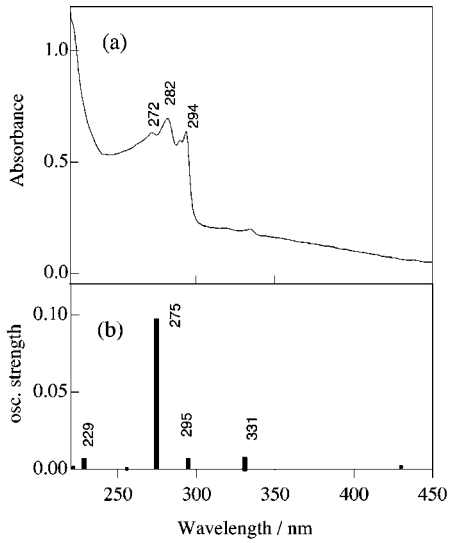

Figure 4. (a) UV−vis absorption spectrum of **4d** observed after complete photolysis of **2d** at 308 nm and (b) TDDFT computational results for **4d**.

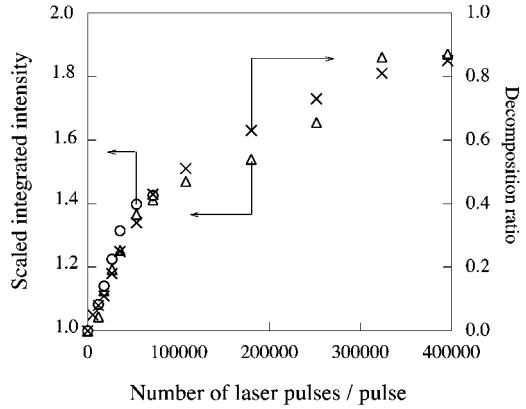

Figure 5. Dynamic behavior of the scaled integrated intensities of the IR bands due to CO_2 (circles, 0−72000 pulses) and CO (triangles), and decomposition ratio of **4a** (crosses) upon irradiation with FHG pulses of a Nd:YAG laser ($\lambda = 266$ nm). The integrated intensities of the CO and CO_2 bands were scaled on the basis of those at the photostationary state upon irradiation at 308 nm. The results for CO_2 are shown only between 0 and 72 000 pulses: because the intensities were too high, the correct intensities of the CO_2 bands could not be estimated after 72 000 pulses.

Figure 6 shows the FTIR spectra of the photoproducts formed upon irradiation at 266 nm. These spectra were obtained by eliminating the IR bands of **4a** from the FTIR spectra observed over the course of the photolysis at 266 nm. This elimination was done by a weighted subtraction using the FTIR spectrum of **4a** obtained at the photostationary state for 308 nm irradiation. The scaling factor (SF) applied in the weighted subtraction corresponds to the molar fraction of the surviving **4a** at the stage.[33] Accordingly, a (1 − SF) value denotes the decomposition ratio of **4a** (see Figure 5). The dynamics of the decomposition ratio almost corresponds to that of both CO and CO_2, indicating that the generated photoproducts were $C_6(CF_3)_2$ species. The observed IR bands of the photoproducts could be classified into two groups on the basis of their dynamic behaviors: (1) IR bands that were observed upon initial irradiation and then gradually decreased and (2) IR bands that were not observed upon initial irradiation but increased over the course of irradiation. The IR band at 1465 cm^{-1}, which is the characteristic IR band of **1a**,[11] belonged to class 1. In addition, IR bands at 797, 1125, 1152, 1166, 1182, and 1239 cm^{-1} were class 1 bands, whereas IR bands at 779, 1141, 1167, 1173, 1206, 1227, 1358, 1381, and 2234 cm^{-1} were class 2 bands. These results revealed that one chemical species was generated in the initial irradiation and then gradually converted into another chemical species. The IR spectra corresponding to these two chemical species can be extracted by applying the weighted subtraction method to the IR spectra observed in the initial and the last stages of the photolysis. Thus, the IR spectrum for class 1 was in good agreement with the theoretical spectrum of **1a**, while the IR spectrum for class 2 was in good agreement with the theoretical spectrum of **6a** (Figure 7). At the UB3LYP/cc-pVTZ level of computation,[30] the asymmetrically coupled C≡C stretching mode in **1a** was predicted to be at 1867 cm^{-1} with an intensity of 5 $km \cdot mol^{-1}$. However, we were not able to observe this weak IR band, probably because it is obscured by C═O stretching bands of the remaining **4a**. The IR band of **1a** corresponding to the band predicted at 606 cm^{-1} overlapped with the band of CO_2 at 662 cm^{-1}, which was confirmed from the temporal increase and decrease of the line width of this IR band during irradiation.

These results indicated that **1a** was initially formed by the photolysis of **4a** and then converted into **6a**. Changes in intensities of the IR bands ascribable to **4a**, **1a**, and **6a** are plotted in Figure 8. The dynamic behaviors of these species revealed that **1a** and **6a** were formed from **4a** following a successive reaction scheme. A detailed analysis of the dynamic behavior of these species is discussed later.

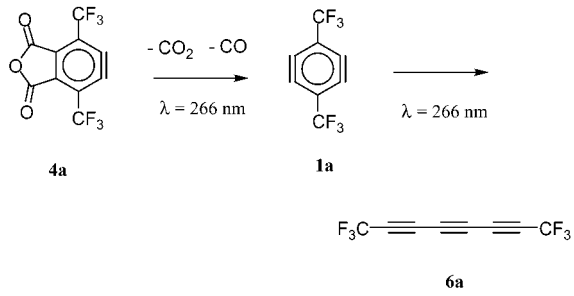

4a **1a** **6a**

In our previous study, the assignment of the IR bands in the C−F stretching region was unclear because several chemical species contributed to the large number of IR bands in this region.[11] In the present study, a more reliable assignment became possible by the separation of the IR spectra of the coexisting chemical species by the weighted subtraction method. The IR bands at 1381, 1358, 1173, 1167, and 1141 cm^{-1} in Figure 7 correspond to those at 1377, 1354, 1176, 1169, and 1139 cm^{-1} in the argon matrix.[11] Although these bands were tentatively assigned to an intermediate species between **1a** and **6a**, they were reassigned to **6a** with the aid of DFT calculations.

3.2.2. Photolysis of (Trifluoromethyl)benzynedicarboxylic Anhydride. In contrast to **1a**, the existence of (trifluoromethyl)-benzdiyne **1c** in the photolysis of benzyne intermediate **4c** was unclear, although the existence of intense IR bands (>200

(33) When the FTIR spectrum of the photoproducts was obtained by weighted subtraction with a scaling factor (SF) of 0.30, 30% of **4a** survived with the remaining 70% being converted into photoproducts. Thus, SF corresponds to the molar fraction of surviving **4a**, while (1-SF) corresponds to the molar fraction of decomposed **4a**, or, equivalently, the total molar ratio of photoproducts generated from **4a**.

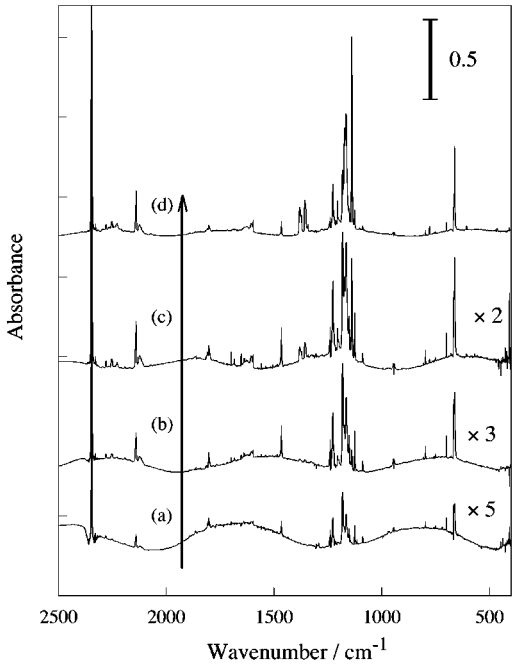

Figure 6. FTIR absorption spectra of photoproducts formed by irradiation of **4a** with FHG pulses of a Nd:YAG laser ($\lambda = 266$ nm): (a) 6000, (b) 27 000, (c) 108 000, and (d) 396 000 pulses. The decomposition ratios of **4a** were estimated as (a) 5, (b) 18, (c) 51, and (d) 85%. IR bands of remaining **4a** were subtracted.

km·mol^{-1}) was predicted for **1c**. As in the case of **1a**, generation of H−C_6−CF_3 species was suggested by the similar dynamic behavior of the IR bands due to CO and CO_2 and the decomposition ratio of **4c** in the photolysis at 266 nm (Figure S6 in the Supporting Information). Figure 9 shows the IR spectra of the photoproducts formed upon irradiation of **4c** at 266 nm together with the calculated IR spectrum of hexatriyne derivative **6c**. As seen in Figure 9, the IR bands of the photoproducts were mainly ascribed to **6c** on the basis of the agreement between the observed and calculated IR spectra. The dynamic behavior of the IR bands ascribed to **6c** was similar to that of the decomposition ratio of **4c**. Therefore, the major photoproduct in the photolysis of **4c** was identified as **6c**.

3.2.3. Photolysis of Benzynedicarboxylic Anhydride and Its Deuterated Isotopomer. In a previous study,[13] only two IR bands due to photoproducts were observed in the 248 nm photolysis of unsubstituted **2b** or dideuterated dianhydride **2b-*d***. These bands were assigned to the C−H(D) bending and stretching modes of the −C≡C−H(D) moiety. In the present study, benzyne intermediates **4b** and **4b-*d*** were photolyzed at 266 nm. Upon irradiation, the IR bands of the −C≡C−H(D) moiety appeared at 642 and 3319 cm^{-1} **4b** and at 504 and 2589 cm^{-1} **4b-*d***. No IR bands ascribable to other photoproducts were observed (Figure S11 in the Supporting Information). Considering that hexatriynes **6a**, **6c**, and **6d** were the final products in the 266 nm photolyses of other systems, these IR bands should be ascribed to hexatriynes. From DFT calculation, these bands are predicted at 555 and 3358 cm^{-1} **6b** and at 428 and 2609 cm^{-1} **6b-*d***. There are no other intense IR bands predicted for **6b** and **6b-*d***. Thus, the obtained photoproducts were ascribed to **6b** and **6b-*d***, respectively on the basis of the good correspondence between the observed and calculated IR spectra. The dynamic behavior of the C−H(D) stretching band corresponds well to the dynamic behavior of the IR band due to CO

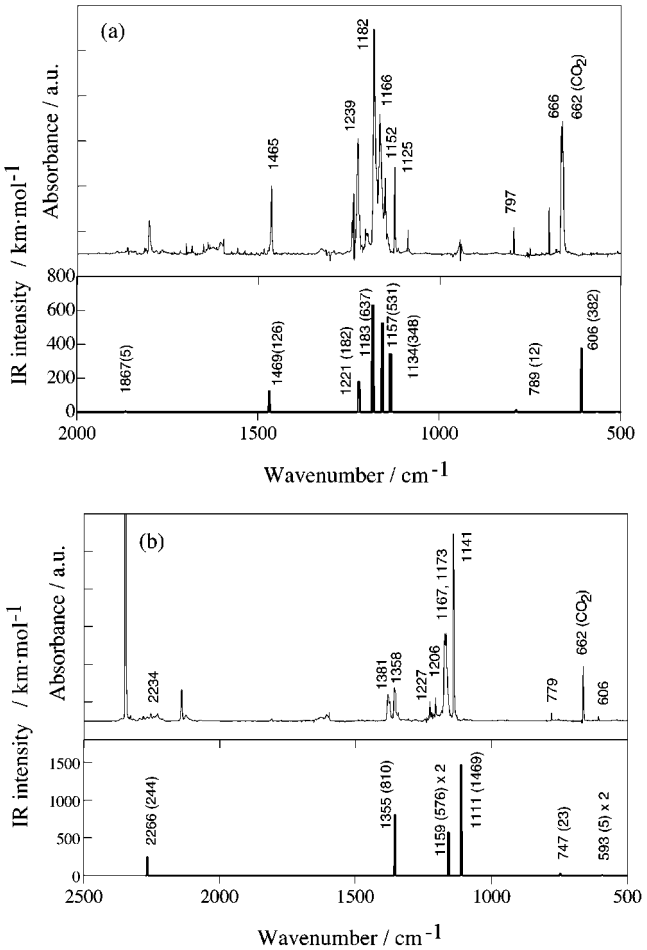

Figure 7. (a) FTIR absorption spectrum of the species for class 1 and theoretical IR spectrum of **1a** calculated at the UB3LYP/cc-pVTZ level. (b) FTIR absorption spectrum of the species for class 2 and theoretical spectrum of **6a** at the B3LYP/6-31G* level.

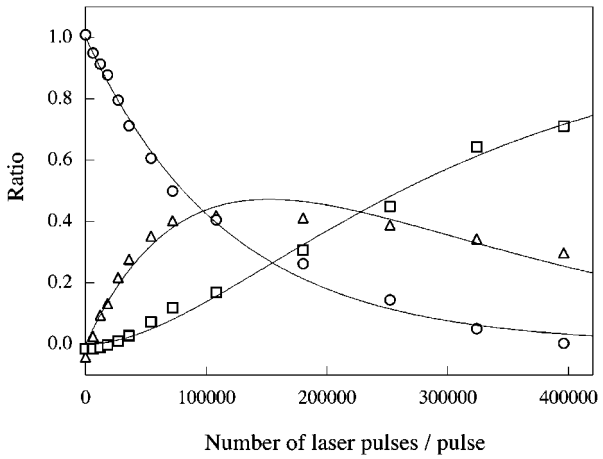

Figure 8. Dynamic behavior of the scaled intensities of the IR bands of **4a** (circles), **1a** (triangles), and **6a** (squares). The IR intensities were scaled on the basis of the parameters estimated in the curve fitting. Curves are fitted results to eqs 1, 2, and 3.

and that of the decomposition ratio of **4b** (**4b-*d***) (Figure S12 in the Supporting Information). These results indicated that the hexatriynes were the major photoproducts in the photolyses.

3.2.4. Photolysis of Difluorobenzynedicarboxylic Anhydride: Direct Observation of Difluorobenzdiyne. In contrast to the other benzyne intermediates, **4d** showed prominent UV−

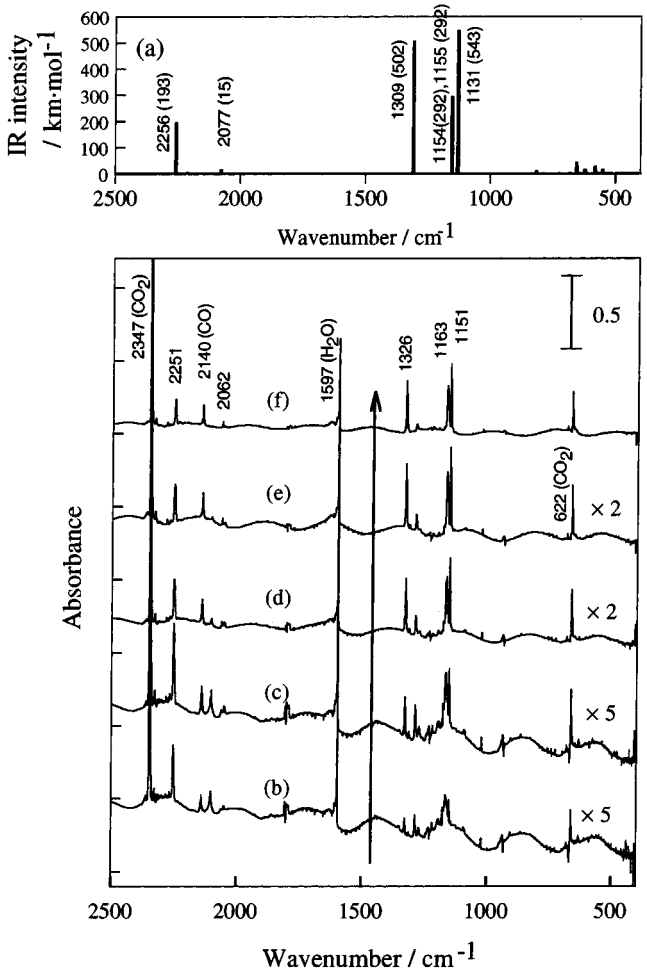

Figure 9. (a) Theoretical IR spectrum of **6c** and observed FTIR absorption spectra of photoproducts formed by irradiation of **4c** with FHG pulses of a Nd:YAG laser ($\lambda = 266$ nm): (b) 18000, (c) 36000, (d) 78000, (e) 144000, and (f) 432000 pulses. The decomposition ratios of **4c** were estimated as (b) 22%, (c) 36%, (d) 62%, (e) 74%, and (f) 93%. IR bands of remaining **4c** were subtracted.

vis absorption bands. Hence, **4d** was more efficiently photolyzed at 266 nm than the other benzyne intermediates. The FTIR spectra of the photoproducts obtained upon irradiation at 266 nm are shown in Figure 10. In the initial photolysis, major IR bands were observed at 579, 929, and 1439 cm^{-1} (Figure 10a). The predicted IR spectrum of **1d** was simple compared to that of **1a** because of the simple chemical structure of **1d**. Therefore, the observed IR bands were ascribed to **1d** with certainty on the basis of good agreement between observed and calculated spectra (Figure 11). In addition to these bands, a weak absorption band at 1174 cm^{-1} was also assigned to **1d** on the basis of the dynamic behavior of the IR bands; this band was also predicted in the theoretical spectrum. Thus the generation of **1d** was confirmed. This is the second benzdiyne derivative that has been directly observed. Although the asymmetrically coupled C≡C stretching mode in **1d** was predicted to be at 1529 cm^{-1} with an intensity of 0.5 km·mol^{-1} (UB3LYP/cc-pVTZ calculation), this IR band could not be observed experimentally, probably because of very low intensity. The IR bands ascribed to **1d** decreased upon continued irradiation at 266 nm, while the IR bands at 830, 875, 1424, and 2322 cm^{-1} increased. These IR bands are in good agreement with those in the calculated IR spectrum of **6d** (Figure 11). Thus, we confirmed that, as was the case for **1a**, ring opening of **1d** upon irradiation at 266 nm led to the formation of **6d**. In addition to the IR bands ascribed to **1d** and **6d**, broad IR bands were observed around 2100 cm^{-1} (Figure 11). Corresponding IR bands were not observed or were very weak in the photolyses of other benzyne intermediates. Bands in this wavenumber region are typical for ketene species. Careful analysis of these bands revealed that there were two IR bands with different dynamic behaviors: a band at 2109 cm^{-1} was replaced by a band at 2129 cm^{-1} during the photolysis, indicating that two ketene species were involved in the photolysis. The dynamic behaviors of these two IR bands indicated that the first ketene species (**k−A**) was formed directly from **4d**, and that the second species (**k−B**) was formed from **1d** or **k−A**. The dynamic behaviors of these IR bands were compared with those of IR bands due to **1d**, **6d**, CO and CO_2 and with the decomposition ratio of **4d**. From the dynamics, we concluded that the amount of **k−A** in the photolysis was not negligible and that **k−B** was a minor product (Figure S19 in the Supporting Information). The reaction scheme for the photolysis of **4d** at 266 nm can be depicted as follows. The present experimental results suggested that neither ketene is analogous to cyclopentadienylideneketene, which is formed from benzyne and CO. Studies directed at identifying these ketenes are in progress, and the details of these studies will be reported elsewhere.

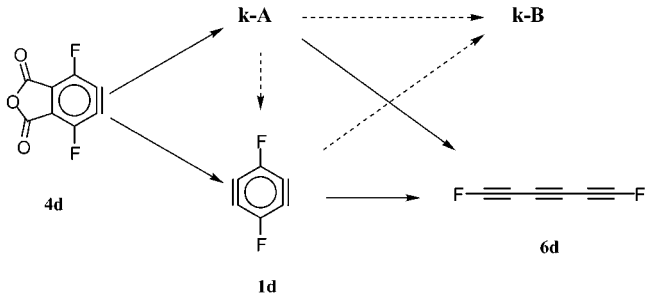

3.3. Calculated Energies for Benzynes, Benzdiynes, and Hexatriynes. Although the reactions from benzynes to hexatriynes are photoinduced processes, the calculated energies of the species involved in the reactions may be helpful for interpreting the different photochemical behaviors observed for the five kinds of derivatives. Figure 12 compares the energies of **2a**, **4a**, and **6a** with the energy of **1a**. These energies were calculated at the B3LYP/6-31G* level and were corrected with scaled zero-point vibrational energies.[31] The energy difference (Δ_1) between benzyne **4a** and benzdiyne **1a** was estimated as 85 kcal·mol^{-1}: this is a rather large value compared to the energy difference between **2a** and **4a** (55 kcalmol^{-1}). This large energy difference (destabilization) and the ring strain in the benzene ring make benzdiyne **1a** highly unstable and susceptible to decomposition by ring opening. The corresponding energy differences for the other derivatives are summarized in Table 1.

In all cases, Δ_1 was estimated as 85−95 kcal·mol^{-1}, indicating that all of the benzdiynes are equally unstable. No remarkable difference was observed between the derivatives in which benzdiynes were detected (**1a** and **1d**) and those in which benzdiynes were not observed (**1b** and **1c**). On the other hand, the energy difference between **1d** and **6d** (Δ_2) was rather small (26 kcal·mol^{-1}) compared to the energy differences for the other three cases. This small difference would come from the

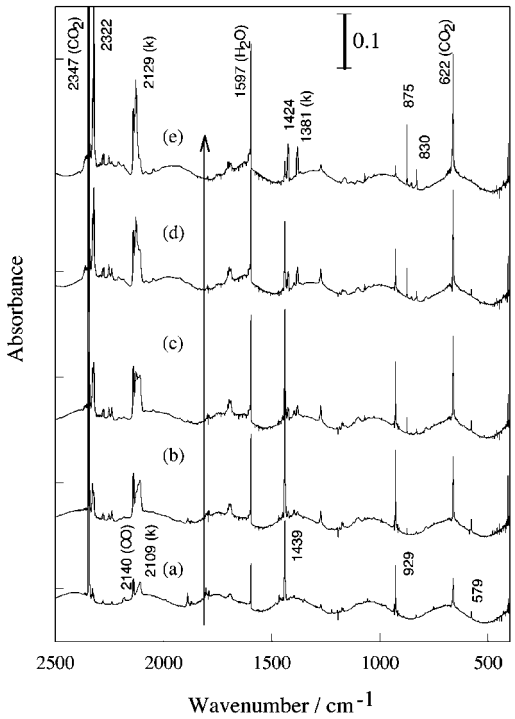

Figure 10. FTIR absorption spectra of photoproducts formed by irradiation of **4d** with FHG pulses of a Nd:YAG laser ($\lambda = 266$ nm): (a) 1200, (b) 4800, (c) 9000, (d) 15,000, and (e) 36,000 pulses. The decomposition ratios of **4d** were estimated as (a) 33%, (b) 69%, (c) 84%, (d) 93%, and (e) 99%. IR bands of remaining **4d** were subtracted. Peaks labeled by (k) are ascribed to ketene species.

resonance effect of the F atoms. In the other three cases, energy differences are similar, indicating that Δ_2 would not affect direct observation of benzdiynes. In a separate report, we will discuss the geometries of benzdiyne derivatives and their relative energies on the basis of a more detailed computational study.[30]

3.4. Analysis of Reaction Dynamics. In the present study, five kinds of benzyne intermediates (**4a**, **4b**, **4b-*d***, **4c**, and **4d**) were obtained by complete photolysis at 308 nm followed by photolysis at 266 nm. Photoreactions at 308 nm (conversion of dianhydrides to benzyne intermediates) were similar, whereas photoreactions at 266 nm were different. In the 266 nm photolyses, only two benzdiynes, **1a** and **1d**, were directly observed. These benzdiynes decomposed upon prolonged irradiation, and hexatriynes were generated as the final products. These results indicated that benzdiyne could be decomposed into hexatriyne by photoinduced ring-opening upon irradiation at 266 nm. Hexatriynes were also the final products in the other three cases. These results indicated that, in all five cases, benzdiyne was generated first and then decomposed into hexatriyne, and that the efficiencies of the decompositions of the benzdiynes depended on the nature of the substituents. From this viewpoint, we analyzed the reaction dynamics of photoconversion of benzyne to hexatriyne.

In the photoconversion of **4a** to **6a**, benzyne intermediate **4a** was first converted into the benzdiyne **1a** and then into hexatriyne **6a**. The dynamics of their IR band intensities (Figure 8) was typical of the dynamics in a successive reaction. The reaction of **4a** to **1a** and the reaction of **1a** to **6a** are not elementary reactions; rather each of these reactions involves several elementary reactions. Nonetheless, the observed dynamics suggested that the reaction dynamics of the 266 nm

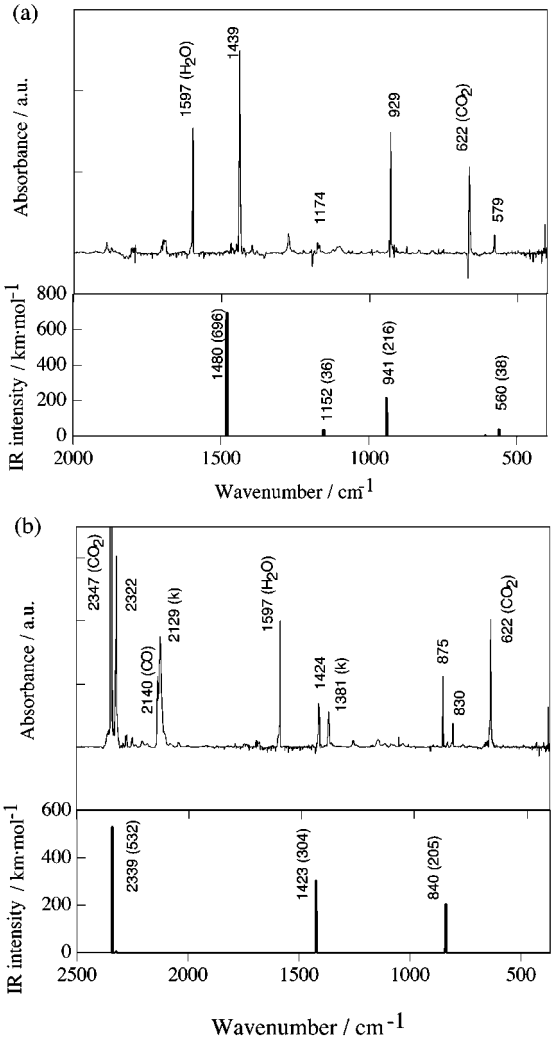

Figure 11. (a) Observed and calculated (UB3LYP/cc-pVTZ) IR spectra of **1d** and (b) observed and calculated (B3LYP/6-31G*) IR spectra of **6d**. Peaks labeled by (k) are ascribed to ketene species.

photolyses could be analyzed as a successive reaction sequence under constant photoirradiation. We analyzed the reaction dynamics of benzyne, benzdiyne, and hexatriyne on the basis of the successive reaction scheme depicted below.

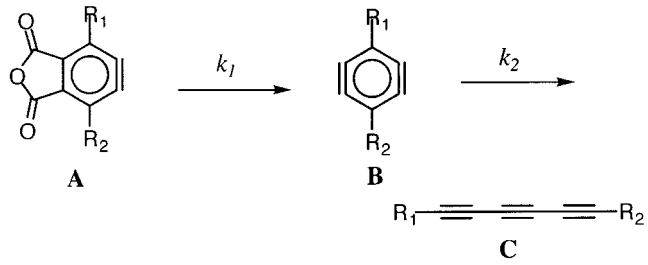

$$[A] = [A]_0 \exp(-k_1 t) \tag{1}$$

$$[B] = \frac{k_1}{k_2 - k_1} \{\exp(-k_1 t) - \exp(-k_2 t)\}[A]_0 \tag{2}$$

$$[C] = \left\{1 + \frac{k_2}{k_1 - k_2} \exp(-k_1 t) - \frac{k_1}{k_1 - k_2} \exp(-k_2 t)\right\}[A]_0 \tag{3}$$

[*A*], [*B*], and [*C*] denote the concentrations of benzyne,

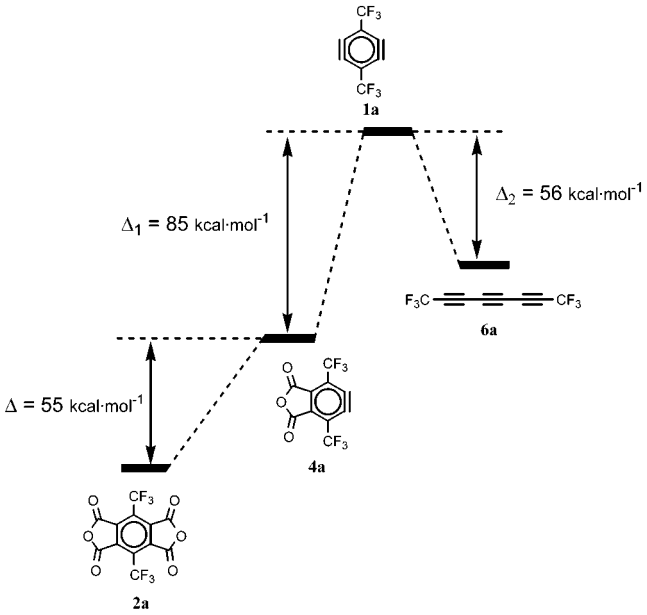

Figure 12. Energy diagram of some of the species involved in the formation of benzyne, benzdiyne, and hexatriyne.

Table 1. Energy Differences between Benzynes and Benzdiynes (Δ_1) and between Benzdiynes and Hexatriynes (Δ_2) Estimated at the B3LYP/6-31G* Level.

compounds	Δ_1 (kcal·mol^{-1})	Δ_2 (kcal·mol^{-1})	benzdiyne
4a − **1a** − **6a**	85	56	observed
4b − **1b** − **6b**	95	53	not observed
4c − **1c** − **6c**	91	51	not observed
4d − **1d** − **6d**	91	26	observed

benzdiyne, and hexatriyne within the matrix, respectively. $[A]_0$ denotes the initial concentration of the benzyne intermediate. The apparent rate constants k_1 and k_2 could be estimated by using eqs 1−3. k_1 and k_2 are not true rate constants: their values depend on the concentration of intermediates, the wavelength and fluence of irradiation, and other experimental conditions. Moreover, it must be noted that all the reactions involved in the generation and decomposition of the benzdiynes are photochemical reactions. Therefore, they should be significantly affected by the absorption coefficients of the benzynes and benzdiynes at the wavelength of laser irradiation. However, none of the benzynes and benzdiynes, except for **4d**,[34] showed prominent absorption bands similar to those observed for **4a** (Figure 1g). In addition, the changes in absorption spectra during the 266 nm photolyses of **4a**, **4b**, and **4c** were slight. Thus, the differences in the absorption coefficients of the benzdiynes were not a major cause of the different photochemical behaviors of these systems. This conclusion was supported by the results of TDDFT calculations (see Supporting Information). IR bands of **4a**, **1a**, and **6a** were analyzed with eqs 1, 2, and 3, respectively, by nonlinear least-squares fitting. First, with eq 1, the k_1 value was estimated to be 8.6×10^{-6} pulse^{-1} from the decay curve of **4a**. Then, with eq 2 the k_2 value was estimated to be 5.0×10^{-6} pulse^{-1} from the dynamics of **1a**. The dynamics of **6a** fitted with eq 3 also gave the same value for k_2. The curves thus obtained fit the experimental values well (Figure 8). Therefore, the reaction from **4a** to **6a** can be expressed as an apparent successive reaction, in which the contributions of other chemical species are negligible. These results indicate that the intermediates in the matrix were in a near-homogeneous environment and that each reaction was unimolecular in nature. In this context, the estimated k_1 and k_2 values represent the total efficiencies of the reaction of **4a** to **1a** and the reaction of **1a** to **6a**. From the curve for **1a**, the maximum yield of **1a** in the matrix was estimated to be 47%. Because the contribution of ketene species was not negligible, the reaction dynamics for **4d** could not be analyzed with eqs 1−3.

In the photolyses of **4b**, **4b-*d***, and **4c**, we found no evidence for chemical species other than those shown in the above successive reaction scheme, although we did not confirm formation of benzdiynes. For these cases, we attempted to use eqs 1 and 3 to analyze the reaction dynamics of the photoconversion of benzynes to hexatriynes (Figures S7 and S13 in the Supporting Information). For **4b**, **4b-*d***, and **4c**, the k_1 values were estimated to be 4.7×10^{-6}, 9.0×10^{-6}, and 9.3×10^{-6} pulse^{-1}, respectively. Next, k_2 values were estimated from the dynamic behavior of the IR band of hexatriyne and eq 3. For **4b-*d*** and **4c**, the k_2 values were estimated to be 1.0×10^{-2} and 7.7×10^{-5} pulse^{-1}, respectively. The obtained dynamics showed that the maximum yields of benzdiynes **1b-*d*** and **1c** were 0.2 and 8.8%, respectively. On the other hand, because $k_2 \gg k_1$, the least-squares fitting did not converge in the case of **4b**. Therefore, the maximum yield of **1b** would be lower than 0.2%. These results show that it is essentially impossible to detect **1b** and **1b-*d*** in the photolysis of **2b** and **2b-*d***, respectively, even if they have intense IR bands. Meanwhile, **1c** should be formed with the maximum yield of 8.8%. When the yield of **1c** was near the maximum, a very weak IR band was observed at 1445 cm^{-1}. This band was ascribed to the characteristic ring deformation mode of the benzdiyne structure (see Supporting Information (Figure S8)).

As described above, the k_1 and k_2 values reflect the total efficiencies of the reaction of **4a** to **1a** and the reaction of **1a** to **6a**. The maximum yield of benzdiyne is high, when the efficiency of benzdiyne decomposition (k_2) is low compared to that of benzdiyne generation (k_1). Therefore, the k_2/k_1 ratio may be used to judge whether benzdiynes could be directly observed. The k_2/k_1 ratios for **1a**, **1b-*d***, and **1c** were estimated to be 0.59, 1.1×10^3, and 8.2, respectively. The corresponding ratio for **1b** would be larger than 1.1×10^3. The k_2/k_1 ratio for **1d** could not be obtained because of a complicated reaction scheme. However, considering that the IR spectrum of **1d** was clearly observed, we can deduce that the k_2/k_1 ratio for **1d** must be low. Thus, a small k_2/k_1 ratio was estimated for disubstituted species compared to the species containing H(D) atoms, implying that the migration of an H(D) atom plays an important role in the increase of the apparent rate constant for the ring-opening reaction. That is to say, the substitution by CF_3 or F groups results in the higher concentration of benzdiynes because the rearrangement and ring-opening reactions are suppressed.

4. Conclusions

We carried out wavelength-selective photolyses of five kinds of benzenetetracarboxylic dianhydride derivatives in the nitrogen matrixes at 13 K. In these photolyses, all dianhydrides were converted into benzyne intermediates upon irradiation at 308 nm. These benzyne intermediates could be further photolyzed

(34) In the photolysis of **4d**, the generated ketenes showed prominent absorption bands that obstructed the absorption spectrum of benzdiyne.

at 266 nm. In the 266 nm photolyses, the generation of only two kinds of benzdiynes, 3,6-bis(trifluoromethyl)-1,4-benzdiyne (**1a**) and 3,6-difluoro-1,4-benzdiyne (**1d**), was confirmed on the basis of good correspondence between the observed and calculated IR spectra. Benzdiyne **1d** is the second trapped benzdiyne to be directly observed after the first, **1a**. Both **1a** and **1d** were converted into hexatriynes upon prolonged irradiation. In the other three cases, only hexatriynes were observed as major photoproducts. These results indicated that the generated benzdiynes could be photolyzed into hexatriynes upon irradiation at 266 nm. The photoconversion of benzyne to hexatriyne could be analyzed by assuming a successive reaction scheme. The ratio of the efficiency for benzdiyne decomposition to that for benzdiyne generation was shown to be useful for judging whether benzdiynes could be directly observed spectroscopically. This ratio was affected by the nature of the substituents. For **1a**, this ratio was estimated to be 0.59, which corresponds to a maximum yield of 47%. The migration of a light H(D) atom plays an important role in increasing the of efficiency of the ring-opening reaction. Suppressing the ring-opening reaction by replacing the H(D) atom with the F or CF_3 group made the direct observation of benzdiynes possible.

Acknowledgment. We are grateful to Dr. Masaya Moriyama (The University of Tokyo) and Dr. Hans P. Reisenauer (Justus-Liebig University) for helpful discussions.

Supporting Information Available: Details of the photolyses of all precursors and computational results (Geometry, calculated and observed frequencies, energy diagram for intermediates, and vibrational modes of benzdiynes) (PDF). This material is available free of charge via the Internet at http://pubs.acs.org.

JA017566N